Proceedings of the 3rd Croatian Conference on Earthquake Engineering - 3CroCEE
19–22 March 2025, Split, Croatia

DOI: https://doi.org/10.5592/CO/3CroCEE.2025.48

EXPERIMENTAL TESTING OF CIRCULAR RC BRIDGE PIER MODELS SUPPORTING REFINED 3D MICRO-MODELING

Laurent Hakaj [(1)], Jelena Ristic [(2)], Toni Arangelovski [(3)], Danilo Ristic[(4)]

[(1)] *PhD student, Faculty of Civil Engineering, Ss. Cyril and Methodius University, Skopje, Republic of North Macedonia, e-mail: laurent.hakaj123@gmail.com*
[(2)] *Assoc. Prof. Dr. Sc., Faculty of Engineering, Department of Civil Engineering, International Balkan University (IBU), Skopje, Republic of North Macedonia, e-mail: risticjelenaibu@gmail.com*
[(3)] *Prof. Dr. Sc., Faculty of Civil Engineering, Ss. Cyril and Methodius University, Skopje, Republic of North Macedonia, e-mail: arangelovskitoni@gf.ukim.edu.mk*
[(4)] *Prof. Dr. Sc., Institute of Earthquake Engineering and Engineering Seismology (IZIIS), Ss. Cyril and Methodius University, Skopje, Republic of North Macedonia, e-mail: danilo.ristic@gmail.com*

Abstract

This paper shows the original results obtained from the realized laboratory tests of nonlinear response of the constructed typical large-scale prototype models of circular RC bridge piers under simulated interactive effects of earthquake-like cyclic horizontal loads and different levels of axial loads. Considering the obtained test results, the most important observations regarding refined analytical modeling and accurate earthquake response analysis of RC bridges can be briefly summarized: (1) The inelastic behaviour of reinforced concrete bridge piers is characterized by a variety of complex influencing phenomena directly resulting from the successive degradation of mechanical properties of the used steel and concrete material. The complex inelastic material response mainly results from the induced complex interactive effects of vertical and horizontal loading. To achieve a realistic analytical simulation of such a complex nonlinear process, the effects of the most important influencing factors should be analytically modeled. This can be achieved through the development of an experimentally proved advanced nonlinear (micro) analytical model based on the results obtained from the conducted representative experimental tests. (2) The presented experimental results indicate that the inelastic behaviour of the tested RC bridge pier models is directly affected by their actual geometry and by the applied level of axial load. The earthquake-induced large time-variation of axial forces in critical bridge piers can introduce complex effects on the overall inelastic structural response. To predict the inelastic earthquake response of specific bridges involving large spans and very tall RC bridge towers, the analytical model should be capable of accounting for the induced instantaneous interactive effects of bending and time-varying axial forces. The development of an advanced nonlinear analytical 3D micro-model to realistically simulate the above-stated complex phenomena represents the specific study objective of the next research phase.

Keywords: bridge, concrete, column, nonlinear response, bending forces, axial forces

1. Introduction

Based on damage observations following strong earthquakes that occurred in the past, it was confirmed that the existing RC bridge piers were commonly exposed to the critical interactive effects of induced cyclic bending and varying axial loads [1-6]. The interactive effects of bending and varying axial loads are particularly relevant and can be critical in the case of modern large-span cable-stayed or cable-suspended bridges having very high RC bridge piers (towers), often constructed with a specific A-shaped geometry [7-10]. Due to this specific axial loading phenomenon, severe damages were also observed to the most frequent regular multi-span RC girder bridges during past earthquakes. These types of bridges are commonly supported by piers with different but harmonized stiffness characteristics, representing a combination of long or flexural failure bridge piers and short or shear failure bridge piers. Heavy damages to bridge structures were recorded almost in all seismic regions worldwide. Different types of damages are evident as shown in many published reports about each

Proceedings of the 3rd Croatian Conference on Earthquake Engineering - 3CroCEE
19–22 March 2025, Split, Croatia

DOI: https://doi.org/10.5592/CO/3CroCEE.2025.48

specific event, for example, the earthquake in Japan [1], the earthquake in Chile [2], the earthquakes in the USA and in China [3], etc.

Renowned research centers worldwide have been performing continuous research toward reducing catastrophic earthquake consequences through the improvement of regulations for the design and construction of structures in seismically active regions [11-17]. Recently, extensive research involving shaking table tests on large-scale models has been conducted by the second and the fourth author and their collaborators, mainly targeted to seismic upgrading of isolated structures with specific energy dissipation devices, [18-24]. Shaking table tests of scaled bridge models have intensively been carried out by many researchers, [25-26], exploring the established, practically applicable model similarity conditions [27].

The presented experimental testing of circular RC bridge pier models was conducted to generate original background experimental data supporting the development of a refined analytical 3D micro-model. The study results will contribute to the improvement of the seismic design and seismic safety of RC columns of common bridges and also of very tall RC towers (often taller than 100 m) supporting large-span cable-stayed or suspended bridges. The presented extensive and original experimental tests of the constructed large-scale circular RC bridge prototype models were performed at the RESIN Laboratory, Skopje, established as a regional research centre by Prof. D. Ristic, (PPD project director), in the framework of the innovative NATO Science for Peace and Security Project: Seismic Upgrading of Bridges in South-East Europe by Innovative Technologies (SFP: 983828).

2. Study Objectives

Bending rarely occurs in reinforced concrete members without axial load being present. In the case of columns, dominant axial loads exist even initially, while very large bending moments can be additionally imposed during structural earthquake response, producing stress-strain state beyond material elastic limit. Reinforced concrete members decrease their stiffness with the development of cracks in concrete and plastic strains in steel. However, many structures could have avoided severe damages or total collapse during past strong earthquakes, with induced loads that were even larger than the design ones, because of the favorable nonlinear characteristics of their reinforced concrete members. To introduce effective and rational earthquake-resistant design of reinforced concrete structures, an understanding of the real inelastic response characteristics of the structural members appears to be essential. The most convenient method to achieve this goal is experimental testing of various reinforced-concrete members under expected loading conditions. The nonlinear behaviour testing is especially useful because the obtained experimental results may be widely applied:

- to evaluate the seismic performances of newly designed reinforced-concrete structural members under realistically simulated expected loading patterns;
- to provide necessary evidence for calibration and improvement of existing seismic design regulations, and
- to generate a sufficient volume of representative experimental data needed for the development and verification of analytical predictive models, etc.

Although numerous experimental investigations were conducted in the past, the urgent need for further experimental studies and advanced analytical modeling of the inelastic behaviour of reinforced-concrete members under various loading conditions has been pointed out by many researchers. To solve complex design problems of modern structures, an advanced analytical model applicable for the realistic simulation of complex inelastic response of reinforced concrete columns is needed. The conducted extensive experimental research was mainly directed to such specific study objectives.

3 Testing of Circular RC Flexural Failure Bridge Pier Models

3.1 Circular RC Flexural Failure Prototype Models

DOI: https://doi.org/10.5592/CO/3CroCEE.2025.48

The presented experimental program involving laboratory testing of reinforced concrete flexural failure (FF) bridge pier models was elaborated based on consideration of various representative design and testing aspects, including: (1) selection of circular cross-section of the piers because it is frequently applied in real bridge structures as a very convenient shape from structural, aesthetic and hydraulic point of view; (2) consideration of long, or flexural failure bridge prototype models (Ml-A and M1-B) because their application is common in bridges located in seismic areas and it is important to experimentally test their inelastic response and failure modes under interactive loads; (3) selection of cantilever type bridge piers for testing, simulating fixation in the footings and hinges at the top, because this type of connection represents the main differences between bridge piers and building columns. In practice, hinge conditions at the top of the piers are usually provided by the installation of bridge bearings, supporting the superstructure mass; (4) consideration of piers' aspect ratio of H/D = 6.22 to investigate the characteristics of the dominant flexural failure during their inelastic response. The symbols D and H represent the pier diameter and distance between the pier fixation level and the level of applied lateral load, respectively; (5) assuming the same design conditions for both tested flexural failure models, M1-A and M1-B including, geometry, concrete class, reinforcement arrangement, laboratory test set-up, etc., to study the effect of different levels of applied axial loads on the hysteretic response of the piers, and (6) design of adequate and identical pin-type mechanisms for application of axial and cyclic lateral loads, and identical fixation system of the footings to provide realistic simulation of loading of the piers in laboratory conditions.

The geometrical properties of the model, the reinforcing steel layout and the designed elements for application of reversed cyclic lateral and compressive vertical load are presented in Fig. 1.

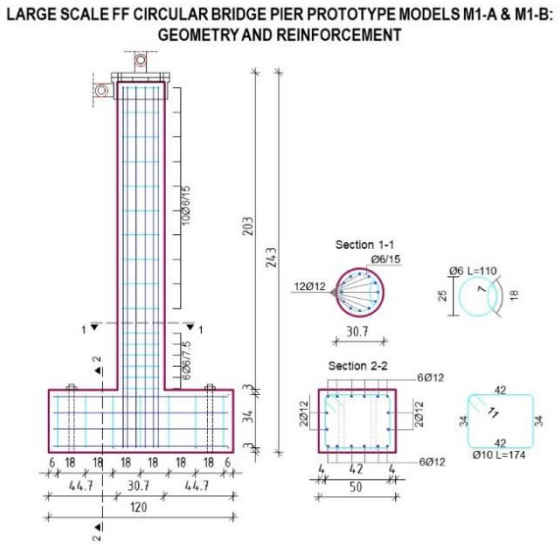

Figure 1. Geometry and reinforcement of the tested flexural failure circular RC bridge pier prototype models M1-A and M1-B.

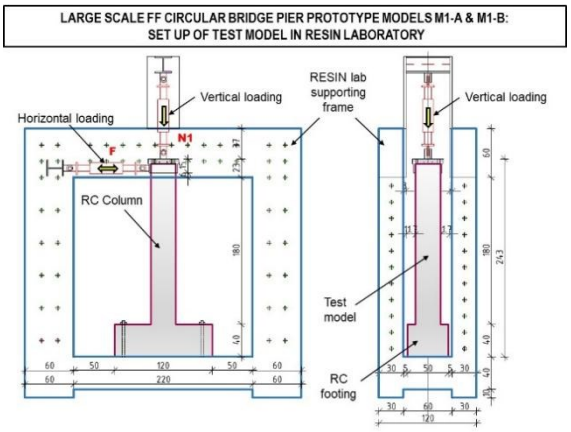

Figure 2. Set-up of flexural failure circular RC bridge pier models M1-A and M1-B in the RESIN laboratory testing frame.

The pier body was designed to be 200 cm in height and 30.7 cm in diameter and be fixed in the reinforced-concrete footing with dimensions 120 x 50 x 40 cm. Four circular holes were provided at both sides of the footing and used to fix it to the laboratory stiff testing frame. A square steel plate, 400 x 400 x 30 mm, was anchored at the top of the pier. In the steel plate, a central hole of 120 mm in diameter was provided for casting of the RC concrete column in a vertical position. Additional four holes ϕ30 mm at the steel plate corners were used for connecting the pin-joint device to the hydraulic actuator for the application of the axial load. A similar pin-joint device was installed between the iron ring placed at the upper end of the pier and the hydraulic actuator for application of reversed lateral force. There was a longitudinal reinforcement of 12 ϕ 12 mm steel bars, grade 240/360, providing a

DOI: https://doi.org/10.5592/CO/3CroCEE.2025.48

percentage of reinforcement of 1.83 in total. Transverse reinforcement was provided by single stirrups (hoops) 6 mm in diameter, placed at a distance of 7.5 cm near the fixed end, the expected plastic hinge region, and at a distance of 15 cm in the remaining part of the pier. The reinforcement of the footings consisted of 16 ϕ 12 mm steel bars, confined by stirrups placed at a distance of 18 cm. The volumetric ratio of the pier transverse reinforcement at the fixed end region was p_s = 0.00395, and half of this was in the remaining part. After arrangement of the reinforcing steel, it was placed in the previously prepared steel forms, equipped with mechanisms for easy assembling and disassembling. Casting of the concrete was carried out in a vertical position and an internal vibrator was used for its compaction. River gravel with a maximum grain size of D = 16 mm was applied, while its remaining characteristics (strength, grain size distribution, etc.) were designed based on the existing design requirements. Portland cement with attested quality was applied for concrete preparation. Concrete compressive strength was determined as an average value of the tested sample cubes proportioned 20 x 20 x 20 cm, taken during the casting of the specimens. The average concrete compressive strength amounted to 45.6 MPa. The typical set-up of the flexural failure circular RC bridge pier models M1-A and M1-B in the RESIN laboratory stiff testing frame is shown in Figure 2.

3.2 Testing Program and Results from Cyclic Tests of FF Prototype Models

For experimental testing of the prototype model M1-A, the laboratory testing frame was used, Fig. 2. The experimental test was carried out under the simulated effect of constant vertical and cyclic horizontal load. As shown in Fig. 1, a vertical compressive load was applied upon the RC column with intensity N1 = 149.0 kN by using the respective hydraulic actuator. A horizontal reversed cyclic load was applied by using the horizontal hydraulic actuator located at the top of the circular RC column model. The loading process upon experimental model M1-A was realized in two loading phases. In the first phase, a vertical load was slowly applied with an incremental increase of loading of the RC column at each successive discrete step. Following the achievement of the assigned constant value of vertical load N1 = 149.0 kN, loading in the second phase was continued by the application of cyclic horizontal loading. The cyclic loading of the model was efficiently provided through the successively applied positive and negative displacement increments, according to the prescribed full history of cyclic displacements. To provide insight into the development of cracks in concrete, very small but well-adjusted displacement increments were applied.

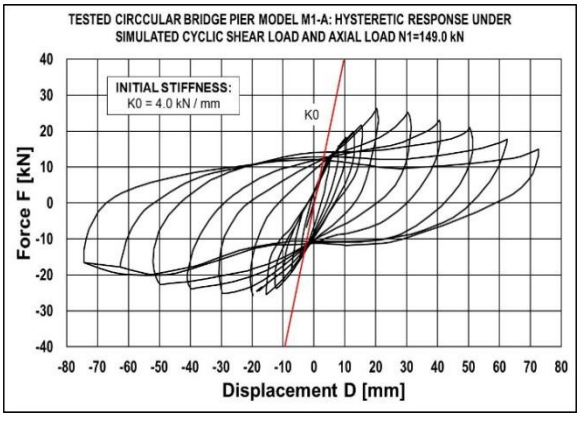

Figure 3. Hysteretic response of RC model M1-A tested under interactive effects of cyclic horizontal and vertical load N1 = 149.0 kN.

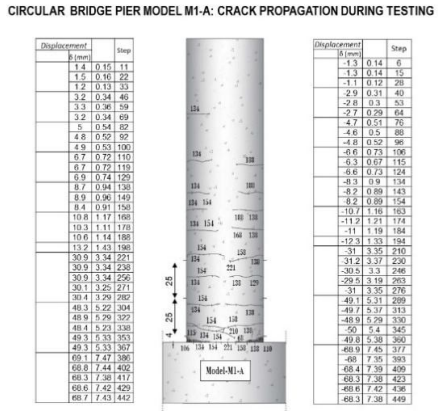

Figure 4. Typical propagation of cracks in concrete during experimental testing of flexural failure RC prototype model M1-A.

During the tests, the applied electronic instrumentation system provided acquisition of a large set of numerical values of measured quantities, including the measured values of displacements Di (mm) and corresponding restoring force Fi (kN) at each loading step. Using the recorded numerical values of force and displacement, the hysteretic nonlinear response of the tested experimental model M1-A was obtained for a quite large range of cyclic deformations, Fig. 3. The obtained hysteretic relationship very successfully represents the real nonlinear response of the tested model considering that almost

DOI: https://doi.org/10.5592/CO/3CroCEE.2025.48

symmetrical hysteretic relationship was obtained in the domain of positive and negative deformations. The resulting hysteretic relationship was used to obtain the representative envelope curve and to successfully define the major envelope segments for the positive and the negative sides with defined characteristic points Y, U and L that were also almost symmetrical, Fig. 7. Point Y represents the yielding point, point U indicates the recorded maximum value of the restoring force F, whereas point L defines the maximum deformation D. Generally, the obtained hysteretic relationship points to a very stable nonlinear response and expected good ductility of the experimentally tested prototype model M1-A. Fig. 4 graphically shows the pattern of the recorded propagation of initial and enlarged cracks in concrete during the experimental testing of flexural failure RC prototype model M1-A.

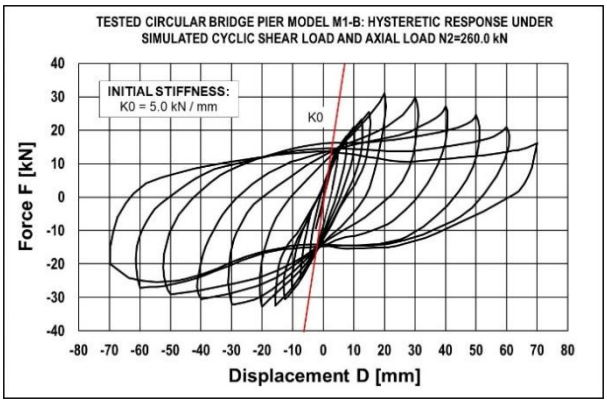

Figure 5. Hysteretic response of RC model M1-B tested under interactive effects of cyclic horizontal and vertical load N2 = 260.0 kN.

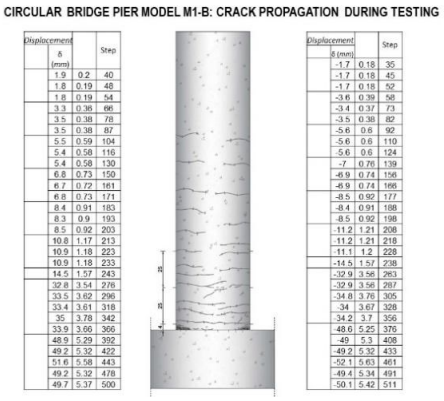

Figure 6. Typical propagation of cracks in concrete during experimental testing of flexural failure RC prototype model M1-B.

Similarly, the loading process upon experimental model M1-B was realized also in two loading phases. After achieving the prescribed larger value of vertical load N2 = 260.0 kN, loading in the second phase was continued with the application of cyclic horizontal loading. Using the recorded time histories of force and displacement, the hysteretic response of the tested experimental model M1-B was obtained and presented in Fig. 5. From the resulting hysteretic relationship, the representative envelope curve was obtained for the positive and the negative displacements with defined characteristic points Y, U and L that were also almost symmetrical, Fig. 7. Fig. 6 graphically shows the crack propagation pattern in concrete during the experimental testing of the flexural failure RC prototype model M1-B.

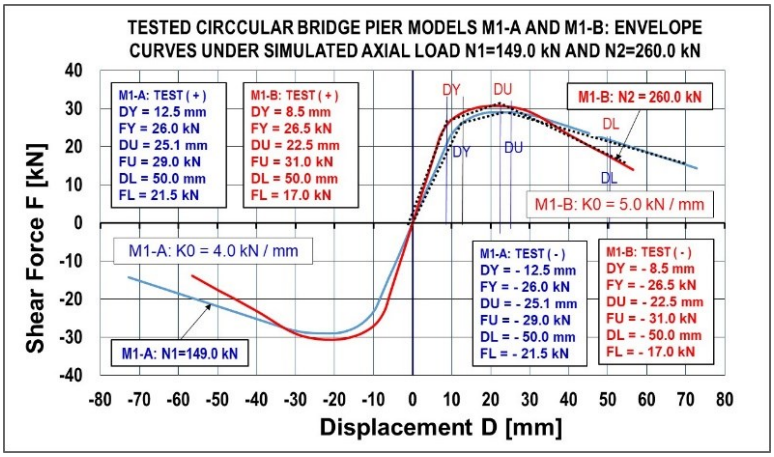

Figure 7. Comparative envelope curves recorded from the tests on models M1-A and M1-B under simulated interactive effects of cyclic horizontal load and vertical loads N1 = 149.0 kN and N2 = 260.0 kN.

DOI: https://doi.org/10.5592/CO/3CroCEE.2025.48

• ***Observation from experimental testing of FF models:*** Based on the original results obtained from the conducted experimental tests on circular RC flexural failure bridge pier prototype models, important observations can be derived. Considering the comparatively presented envelope curves in Fig. 7 for the tested FF models M1-A and M1-B under simulated interactive effects of cyclic horizontal and vertical loads at two levels, N1 = 149.0 kN and N2 = 260.0 kN, significant differences are evident.

(a) The plotted load-displacement hysteretic relationships for both flexural failure (FF) specimens indicate a recorded greater initial stiffness and larger lateral load-carrying capacity of the model tested under higher axial load.

(b) However, in the range characterized by imposed larger displacement, typical for structural response due to strong ground motion, a higher applied axial load produced more intensive degradation of the model ductility and ultimate lateral load carrying capacity.

(c) The observation mentioned under (b) points out the high importance of taking into account the actual level of the imposed axial loads in the analysis of the inelastic earthquake response of reinforced concrete structures. This is especially important for structures exposed to severe earthquakes when during large inelastic deformations, there is a high variation of axial forces.

(d) The experimental results show that the inelastic behaviour of the critical cross-sections can be greatly affected by the level of applied axial load. The resulting moment-curvature relationship for the critical cross-sections will show a similar tendency as the previously presented one for the load - displacement response. Then, in practice, it is equally important to calculate the hysteretic response of the RC sections considering the interactive effects of bending and varying axial loads.

(e) The change in axial load mainly influences the inelastic responses of the RC columns due to the following two effects: (1) the effect of the initially induced different stress-strain state in concrete and reinforcing steel, and (2) the effect of the induced additional moment along the member due to the imposed lateral displacement, commonly referred to as the P-delta effect.

(f) During nonlinear cyclic tests of circular RC flexural failure bridge pier models, the orientation of the cracks in concrete in a horizontal direction was generally recorded. The recorded generally horizontal cracks mainly resulted from the dominant effect of bending loads.

4 Testing of Circular RC Shear Failure Bridge Pier Models

4.1 Circular RC Shear Failure Prototype Models

The second experimental program involving laboratory testing of reinforced concrete shear failure (SF) bridge pier models was elaborated based on consideration of identical all basic design parameters.

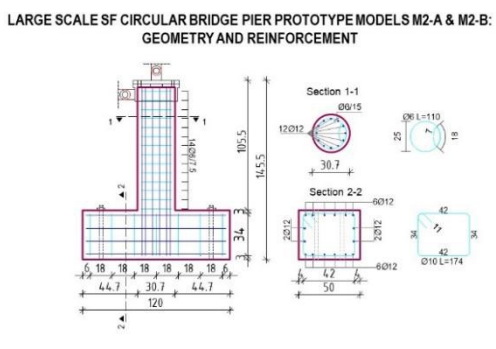

Figure 8. Geometry and reinforcement of the tested shear failure circular RC bridge pier prototype. Models M2-A and M2-B.

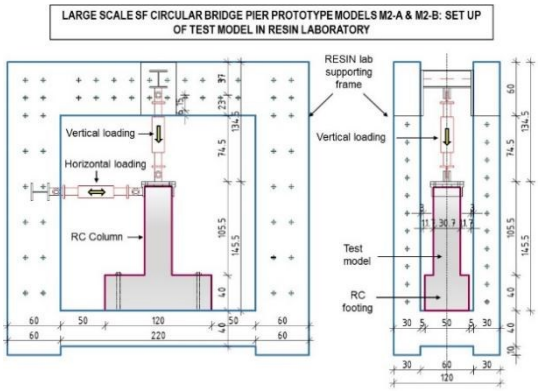

Figure 9. Set-up of the shear failure circular RC bridge pier models M2-A and M2-B in the RESIN laboratory testing frame.

DOI: https://doi.org/10.5592/CO/3CroCEE.2025.48

Actually, the pier geometry, concrete class, reinforcement arrangement and laboratory test set-up were considered identical to provide conditions to evaluate the effect of the defined identical set of different levels of applied axial loads on hysteretic response. However, for comparative purposes, in the design of short or shear failure bridge prototype models (M2-A and M2-B), only their different height was considered, Fig. 8. The typical set-up of shear failure circular RC bridge pier models M2-A and M2-B is shown in Fig. 9. The term shear failure models refers to short piers where, besides flexural deformations, shear deformations produce a very significant effect on their hysteretic response.

4.2 Testing Program and Results from Cyclic Tests of SF Prototype Models

To perform experimental testing of prototype models M2-A and M2-B, the respective connections and the laboratory testing frame were properly adjusted and used, Fig. 9. The first experimental test of prototype models M2-A, representing shear failure specimens, was carried out under the simulated effect of constant vertical and cyclic horizontal load. The vertical compressive load upon the RC column model M2-A was applied with lower intensity N1 = 149.0 kN using the respective hydraulic actuator. Using the recorded time histories of force and displacement, the hysteretic nonlinear response of the tested experimental model M2-A was obtained and it is presented in Fig. 10.

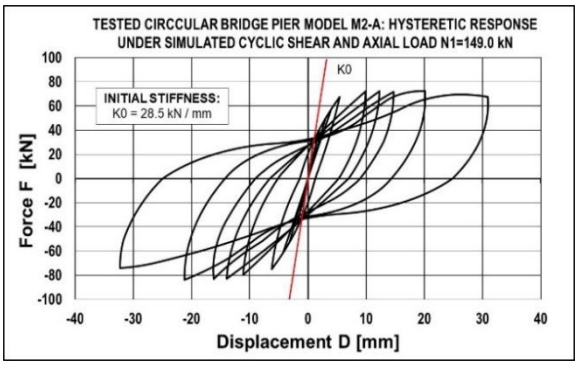

Figure 10. Hysteretic response of RC model M2-A tested under interactive effects of cyclic horizontal and vertical load N1 = 149.0 kN.

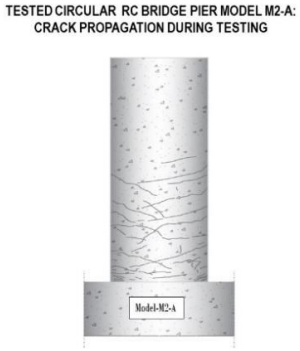

Figure 11. Typical propagation of cracks in concrete during experimental testing of shear failure RC prototype model M2-A.

The resulting, nearly symmetrical hysteretic relationship was used to define the representative envelope curve with the respective characteristic points Y, U and L that were also almost symmetrical, Fig. 14. Fig. 11 graphically shows the pattern of the recorded cracks in concrete during the experimental testing of the shear failure RC prototype model M2-A.

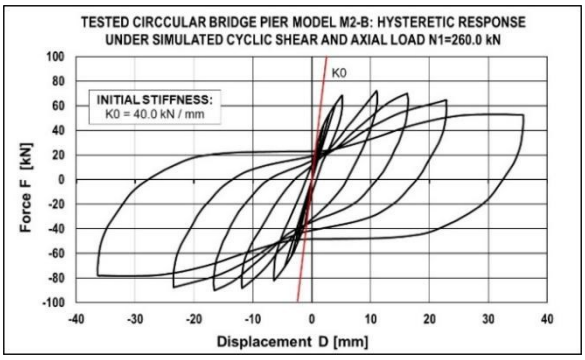

Figure 12. Hysteretic response of RC model M2-A tested under interactive effects of cyclic horizontal and vertical load N1 = 149.0 kN.

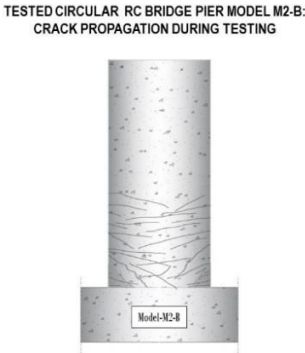

Figure 13. Typical propagation of cracks in concrete during experimental testing of shear failure RC prototype model M2-A.

DOI: https://doi.org/10.5592/CO/3CroCEE.2025.48

The recorded pattern of cracks in this case is very complex due to the complex mixed effect of bending and shear deformations. Analogously, the loading process upon experimental model M2-B was realized also in two loading phases. After the prescribed larger value of vertical load N2 = 260.0 kN was applied, loading in the second phase was continued with the application of cyclic horizontal loading. Using the recorded time histories of force and displacement, the hysteretic response of the tested experimental model M2-B was obtained and it is presented in Fig. 12. From the resulting hysteretic relationship, the representative envelope curve was obtained for the positive and the negative displacements with defined characteristic points Y, U and L that were also almost symmetrical, Fig. 14. Fig. 13 graphically shows the crack pattern recorded during testing of the RC shear failure prototype model M2-B.

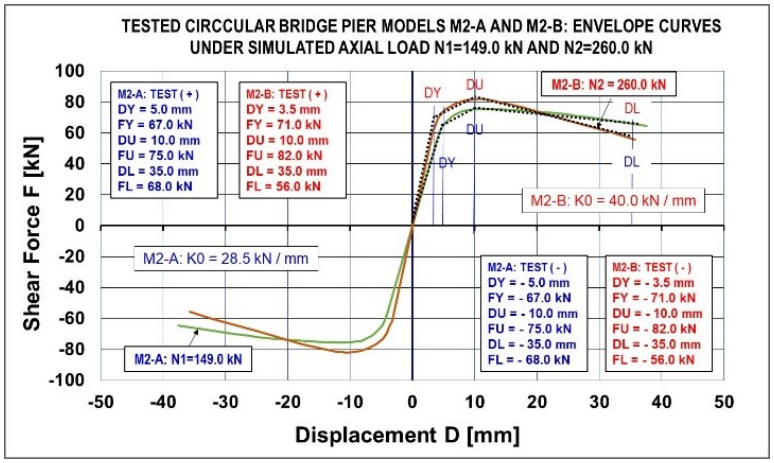

Figure 14. Comparative envelope curves recorded from the tests on models M2-A and M2-B under simulated interactive effects of cyclic horizontal load and vertical loads N1 = 149.0 kN and N2 = 260.0 kN.

• ***Observation from experimental testing of SF models:*** Considering the results obtained from the experimental testing of circular RC shear failure bridge piers prototype models, respective conclusions were drawn. From the comparatively presented envelope curves in Fig, 14, for models M2-A and M2-B tested under simulated cyclic horizontal and vertical loads at two levels, N1 = 149.0 kN and N2 = 260.0 kN, significant differences were also recorded.

(a) The presented load - displacement relationships for both tested shear failure models in Fig. 14, clearly indicate a greater initial stiffness and a larger lateral load carrying capacity in the case of the specimen tested under higher axial load.

(b) However, in the domain characterized with larger displacements, the higher applied axial load produced more intensive degradation of the lateral load capacity. This is specifically important in the cases where the induced inelastic deformations are large and the variation of axial forces is high.

(c) The experimental results show that the effect of shear deformations in this case is very significant, since a very complex pattern of cracks was recorded. Therefore, the commonly computed moment-curvature relationship for the critical cross-sections will be incorrect.

(d) The change in axial load and height of the specimens mainly influences the inelastic responses of the SF models due to the following effects: (1) the effect of the initially induced different stress-strain state in concrete and reinforcing steel, and (2) the effect of the induced large shear deformations due to the effective shear force.

(d) During nonlinear cyclic tests of circular RC shear failure bridge pier models, a complex orientation of cracks was recorded. Suh complex pattern of cracks mainly resulted from the dominant integrative effect of shear and bending deformations.

DOI: https://doi.org/10.5592/CO/3CroCEE.2025.48

• ***Observation from experimental testing of FF and SF models:*** Considering the integral results obtained from the conducted experimental testing of RC flexural failure and shear failure bridge pier prototype models, very important observations were made. From the comparatively presented envelope curves in Fig, 15, for the FF models M1-A and M1-B and for the SF model M2-A and M2-B tested under simulated cyclic horizontal and different vertical loads N1 = 149.0 kN and N2 = 260.0 kN, very significant differences were recorded.

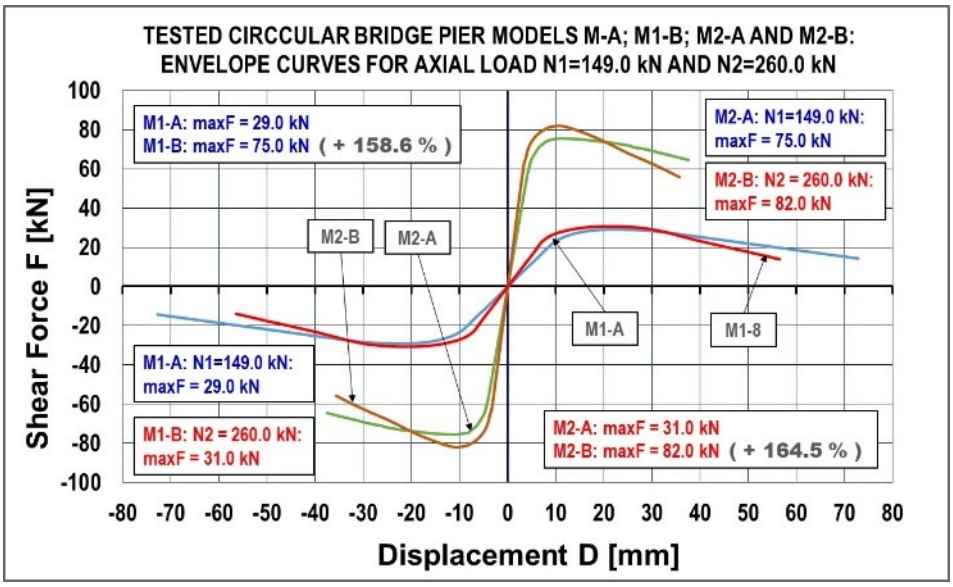

Figure 15. Comparative overview of the recorded nonlinear envelope curves from the experimentally tested flexural failure and shear failure RC bridge pier prototype models under simulated effects of cyclic horizontal and different levels of vertical loads N1 = 149.0 kN and N2 = 260.0 kN

The presented original experimental results obtained from the conducted extensive laboratory tests on large-scale RC flexural and shear failure bridge pier models are directly expressing the high importance of the presented extensive experimental research. Derived from the conducted experimental study was an essential experimental database needed for advancing modern practical applications and for the development of advanced nonlinear analytical micro-models.

5 Conclusions

Analyzing the comparatively obtained original experimental results from the performed experimental testing of circular RC flexural failure and shear failure bridge pier models, several very important conclusions are drawn: (1) The recorded hysteretic responses of the FF bridge pier models show a very good symmetry, stable hysteretic cyclic curves and very good ductility. The hysteretic relationships of the model tested under higher axial load indicate a greater initial stiffness and a larger lateral load capacity. However, in the range of larger displacement, the higher axial load produced more intensive degradation of the model ductility and ultimate lateral load carrying capacity; (2) The hysteretic responses of the SF bridge pier models show a similar behaviour tendency. The envelope curve of the model tested under a higher axial load also indicates a greater initial stiffness and a larger lateral load capacity, but in the range of the larger displacement, the higher axial load produced more intensive degradation of the ductility and lateral load-bearing capacity. However, compared to the FF models, the tested SF bridge pier models showed a much higher lateral load-bearing capacity ranging up to 164.5 %. (3) The recorded initial stiffness of the FF and SF bridge pier models was continuously reduced with the increase of deformations and became increasingly smaller during larger deformations, reaching the zero value at point “U”. The repeated cyclic curves evidently show the regularity of the stiffness deterioration regarding the repeated segments of loading and unloading; (4) The first initiation and

DOI: https://doi.org/10.5592/CO/3CroCEE.2025.48

propagation of cracks in the tested FF bridge pier models occur in the critical tension zones located in the segments close to the fixations of the columns into the RC foundation. During the experimental tests of the prototype models M1-A and M1-B, nearly identical wider zones of occurrence of cracks in concrete were recorded. The orientation of the cracks in this case was dominantly horizontal; (5) In the case of the tested SF bridge pier models, the propagation of cracks occurred with different patterns but also in critical zones located close to the fixations of the columns into the RC foundation. During the experimental tests of the prototype models M2-A and M2-B, similar wider zones of occurrence of cracks in concrete were recorded. The orientation of cracks, in this case, was very complex due to the dominant effect of shear deformations; (6) The obtained original experimental results regarding the nonlinear behaviour characteristics of the tested RC circular FF and SF bridge pier prototype models represent a unique and harmonized database of great importance for experimental validation of the formulated advanced nonlinear analytical micro-models.

Acknowledgements

The experimental tests of the constructed large-scale circular RC bridge prototype models were performed in the RESIN Laboratory, Skopje, established as a regional research centre by Prof. Danilo Ristic, PPD, in the framework of the innovative NATO Science for Peace and Security Project: *Seismic Upgrading of Bridges in South-East Europe by Innovative Technologies (SFP: 983828).* The authors express sincere thanks for the extended cooperation in the testing research.

REFERENCES

[1] Kazuhiko Kawashima, Kenji Kosa, Yoshikazu Takahashi, Mitsuyoshi Akiyama, Tsutomu Nishioka, Gakuho Watanabe, Hirohisa Koga, and Hiroshi Matsuzaki (2011) Damage of Bridges During 2011 Great East Japan Earthquake.

[2] Denis Mitchell, Sharlie Huffman, Robert Tremblay, Murat Saatcioglu, Dan Palermo, René Tinawi, and David Lau. (2010) Damage to Bridges due to the 27 February 2010 Chile Earthquake1, Accepted 5 April 2012: www.nrcresearchpress.com/cjce on June 2012

[3] Wang, Z.; Lee, G.C. A Comparative Study of Bridge Damage Due to the Wenchuan, Northridge, Loma Prieta and San Fernando Earthquakes. Earthq. Eng. Eng. Vib. 2009, 8, 251–261. [CrossRef]

[4] Hashimoto, S.; Abe, M.; Fujino, Y. Damage Analysis of Hanshin Expressway Viaducts during 1995 Kobe Earthquake. III: Three-Span Continuous Girder Bridges. J. Bridge Eng. 2005, 10, 61–68. [CrossRef]

[5] Han, Q.; Du, X.; Liu, J.; Li, Z.; Li, L.; Zhao, J. Seismic Damage of Highway Bridges during the 2008 Wenchuan Earthquake. Earthq. Eng. Eng. Vib. 2009, 8, 263–273. [CrossRef]

[6] Wotherspoon, L.; Bradshaw, A.; Green, R.; Wood, C.; Palermo, A.; Cubrinovski, M.; Bradley, B. Performance of Bridges during the 2010 Darfield and 2011 Christchurch Earthquakes. Seismol. Res. Lett. 2011, 82, 950–964. [CrossRef]

[7] Zhu, J.; Zhang, W.; Zheng, K.F.; Li, H.G. Seismic Design of a Long-Span Cable-Stayed Bridge with Fluid Viscous Dampers. Pract. Period. Struct. Des. Constr. 2016, 21, 04015006. [CrossRef]

[8] Li, X.; Li, J.; Zhang, X.; Gao, J.; Zhang, C. Simplified Analysis of Cable-Stayed Bridges with Longitudinal Viscous Dampers. ECAM 2020, 27, 1993–2022. [CrossRef]

[9] Xu, Y.; Tong, C.; Li, J. Simplified Calculation Method for Supplemental Viscous Dampers of Cable-Stayed Bridges under Near-Fault Ground Motions. J. Earthq. Eng. 2021, 25, 65–81. [CrossRef]

[10] Abdel Raheem, S.E.; Hayashikawa, T.; Dorka, U. Ground Motion Spatial Variability Effects on Seismic Response Control of Cable-Stayed Bridges. Earthq. Eng. Eng. Vib. 2011, 10, 37–49. [CrossRef]

[11] Nigel Hewson and Gerard Parke, (2008) ICE Manual of Bridge Engineering, Second Edition, Published by Thomas Telford Ltd, 1 Heron Quay, London E14 4JD, UK. www.thomastelford.com.

[12] American Association of State Highway and Transportation Officials. AASHTO Guide Specifications for LRFD Seismic Bridge Design, 2nd ed.; American Association of State Highway and Transportation Officials: Washington, DC, USA, 2011; ISBN978-1-56051-521-0.

DOI: https://doi.org/10.5592/CO/3CroCEE.2025.48

[13] Chen, W. F. and Duan, L. [2000] Bridge Engineering, Handbook (CRC Press).

[14] EC8 [1994] Eurocode 8 Design Provisions for Earthquake Resistence of Structures — Part 1-1: Seismic Actions and General Requirements of Structures, ENV 1998-1-1; Part 2: Bridges, ENV 1998-2, Comite Europeen de Normalisation, Brussels.

[15] Wilson, E.L. Three-Dimensional Static and Dynamic Analysis of Structures; Computers and Structures: Walnut Creek, CA, USA, 2001.

[16] Xiang, N.; Goto, Y.; Obata, M.; Alam, M.S. Passive Seismic Unseating Prevention Strategies Implemented in Highway Bridges: A State-of-the-Art Review. Eng. Struct. 2019, 194, 77–93. [CrossRef]

[17] Kowalsky, M. J. and Priestley, M. J. N. [2000] "Improved Analytical Model for Shear Strength of Circular Reinforced Concrete Columns in Seismic Regions," ACI Structural Journal 97(3), 388–396

[18] Ristic, J., Misini, M., Ristic, D., Guri, Z., Pllana, N. (2017): Seismic Upgrading of Isolated Bridges with SF-ED Devices: Shaking Table Tests of Large-Scale Model, *Gradjevinar*, 2147-2017. [DOI]

[19] Ristic, J., Brujic, Z., Ristic, D., Folic, R., Boskovic, M. (2021): Upgrading of Isolated Bridges with Space-Bar Energy-Dissipation Devices: Shaking Table Test, Advances in Structural Engineering, June 23, 2021; pp. 2948–2965.

[20] Ristic, J. (2016): Modern Technology for Seismic Protection of Bridge Structures Applying Advanced System for Modification of Earthquake Response, PhD Thesis, Institute of Earthquake Engineering and Engineering Seismology (IZIIS), "SS Cyril and Methodius" University, Skopje, Macedonia.

[21] Ristic, D. (1988): Nonlinear Behavior and Stress-Strain Based Modeling of Reinforced Concrete Structures under Earthquake Induced Bending and Varying Axial Loads, Doctoral Dissertation, School of Civil Engineering, Kyoto University, Japan.

[22] Ristic, D., Ristic J. (2012): Advanced Integrated 2G3 Response Modification Method for Seismic Upgrading of New and Existing Bridges, 15th World Conf. on Earthquake Engineering, (WCEE), Lisbon.

[23] Ristic, J., Ristic D., Behrami, R., Hristovski, V., (2024): Adaptive Seismic Upgrading of Isolated Bridges with C-Gapped Devices: Model Testing, Civil Engineering Journal, Vol. 10, No. 09, September, 2024.

[24] Ristic, J., Veseli V., Misini, L., Ristic, D., (2023): Seismic Potection of Masonry and Infilled Frame Buildings Using Upgraded Sliding Isolation System with SF Devices, Proceedings of the 2nd Croatian Conference on Earthquake Engineering - 2CroCEE, Zagreb, Croatia - March 22 to 24, 2023.

[25] Guo, W.; Li, J.; Guan, Z. Shake Table Test on a Long-Span Cable-Stayed Bridge with Viscous Dampers Considering Wave Passage Effects. J. Bridge Eng. 2021, 26, 04020118. [CrossRef]

[26] H. Sun, B. Li, K. Bi, N. Chouw, J. W. Butterworth and H. Hao, (2011) Shake Table Test of a Three-Span Bridge Model, Proceedings of the Ninth Pacific Conference on Earthquake Engineering, Auckland, New Zealand.

[27] Candeias, P., Costa, A. C., Coelho, E. (2004): Shaking Table Tests of 1:3 Reduced Scale Models of Four-Story Unreinforced Masonry Buildings, 13th World Conference on Earthquake Engineering, Vancouver, Paper: 2199.